# 5 Exchange splitting as a sensor for magnetization

In the previous chapter, 2PPE was used to study the initial states with respect to their spin polarization, symmetry representation, and as far as possible also their surface character. This chapter focuses now on the intermediate states, in our case the image-potential states. Their character of being a sensor state will be demonstrated by the dependence of the exchange splitting on the underlying material system and the temperature.

## 5.1 Material dependence

As discussed in Section 4.1, the spin-dependent binding energy, which leads to an exchange splitting, is beside the spin polarization the most remarkable feature one realizes by inspecting a spin-resolved 2PPE spectrum as shown e.g in Figure 4.2. The values for the sample work-function, the binding energies and the exchange splitting of image-potential states on 3 ML Fe/Cu(100) and 6 ML Co/Cu(100) are given in Table 5.1.

The binding energy should be independent of the excitation process in 2PPE because it is simply defined by the image potential. However, an influence of the density of initial states can indeed be observed, especially if it exhibits large variations. As discussed in Section 2.2, optical Bloch equations reveal that initial states may still be excited off-resonantly. This process is enhanced when the virtual intermediate state is close to real states, like the image-potential states. Its signal decreases faster with pump-probe delay compared to that of the image-potential states, but contributes at zero delay significantly to the spectrum. In case of a strong inhomogenous distribution of initial states, this leads to a superimposed intensity variation in the 2PPE spectrum. Thus the peak, which is usually solely assigned to the image-potential state, might be shifted and an erroneous determination of binding energy and therefore also of the exchange splitting is likely. This causes also a dependence of the measured exchange splitting on the pump-pulse polarization and in the case of Co/Cu(100) even on the magnetization direction.

There is, however, a way to avoid this problem. For a high delay of the pump and probe pulse the off-resonant contribution becomes negligible and the

| | 3 ML Fe/Cu(100) | 6 ML Co/Cu(100) |
|---|---|---|
| $\phi$ (eV) | 4.76 ±0.03 | 4.74 ±0.03 |
| $-(E^{\uparrow}_{n=1} - E_{vac})$ (meV) | 715±10 | 621±10 |
| $-(E^{\downarrow}_{n=1} - E_{vac})$ (meV) | 659±10 | 595±10 |
| $-(E^{\uparrow}_{n=2} - E_{vac})$ (meV) | 201±7 | 186±7 |
| $-(E^{\downarrow}_{n=2} - E_{vac})$ (meV) | 194±7 | 180±7 |
| $\Delta E_{n=1}$ (meV) | 56±10 | 26±5 |
| $\Delta E_{n=2}$ (meV) | 7±3 | 6±3 |

**Table 5.1**: *Material dependence of the exchange splitting. The binding energy and exchange splitting refer to room temperature grown 3 ML Fe/Cu(100) and 6 ML Co/Cu(100). For iron the measurement temperature was 100 K and for cobalt 300 K, which is for both systems well below the Curie temperature. The error given for the binding energy and the exchange splitting corresponds to deviations for different preparations and an uncertainty of the Sherman function. A systematic error of 25 meV in the binding energy has to be assumed for the uncertainty in zero kinetic energy.*

true binding energy can be determined. This can also be adequately modeled by optical Bloch equations [*Schmidt*, 2007]. The presented binding energies are therefore obtained at a delay larger than 100 fs. The binding energy of the $n$=1 and even the $n$=2 image-potential states can be deduced directly from energy-resolved measurements. Access to the spin-dependent binding energy of IPS with $n \geq 3$ is also indirectly possible by time-resolved measurements due to interference effects known as quantum beats [*Höfer et al.*, 1997]. This will be explicitly shown by [*Schmidt*, 2007].

Let us come back to our results. The work function of 3 ML Fe/Cu(100) is slightly larger compared to results from previous 2PPE measurements which obtained 4.71 eV [*Thomann et al.*, 1999] and 4.68 eV [*Wallauer and Fauster*, 1996]. We can only speculate about the origin of this difference. One reason would be possible little deviations in the preparation or a slight contamination of the film. One has to keep in mind that ultrathin iron films are known to be very sensitive on preparation as discussed in Chapter 2.3.1. For cobalt thin films the work function is slightly smaller than literature values (4.78 eV [*Wallauer and Fauster*, 1996], 4.77 eV [*Thomann*, 1999]).

The binding energy of image-potential states for cobalt thin films is roughly similar to the binding energy for clean Cu(100), whereas generally higher values are obtained for the fcc iron films. This is at odds with the values expected from a one dimensional scattering model where spin-averaged band edges were used [*Wallauer and Fauster*, 1996]. These calculations predict smaller binding energies with respect to the vacuum level for Fe/Cu(100) than for Cu(100). Different values for binding energies as expected from simple theoretical calculations which only consider the band gap situation have also been observed for other ferromagnetic materials and are ascribed to the influence of the $d$ bands at the Fermi level

[*Fauster and Steinmann*, 1995]. Literature values are consistent to the values for cobalt whereas for 3 ML Fe/Cu(100) about 100 meV lower binding energies for the $n$=1 image-potential state are reported [*Wallauer and Fauster*, 1996, *Thomann*, 1999]. This discrepancy might have the same reason as the deviation of the work function.

Let us now focus on the main result of this section, the exchange splitting of both the $n$=1 and $n$=2 image-potential states. Naively one would expect a proportionality of the splitting with the overlap of the wave function to the bulk, which scales with $\Delta E_n \propto n^{-3}$. This has indeed been proven by calculations for Fe(110) using spin-polarized near-surface embedding [*Nekovee et al.*, 1993]. Our results for 3 ML Fe/Cu(100) reflect the $n^{-3}$ dependence. For 6 ML Co/Cu(100) a deviation of almost a factor 2 becomes obvious, which is nevertheless still within the experimental error. At this point it has to be remarked that these are the first results of binding energies of the $n$=2 image-potential state. Other techniques, like spin-resolved inverse photoemission or spin-integrated 2PPE could only determine the exchange splitting of the $n$=1 state. For a complete survey of exchange splitting of image-potential states the reader is referred to [*Donath et al.*, 2007].

*Thomann et al.* [1999] deduced the exchange splitting of the $n$=1 state for 3 ML Fe/Cu(100) to be about 70 meV from spin-integrated 2PPE with two different light polarizations, a technique which is in detail discussed in the Section 5.2.2. The literature values for the exchange splitting of ultrathin cobalt films, which were also obtained with spin-integrated 2PPE, are also larger than the values presented in this work. *Wallauer and Fauster* [1996] determined an exchange splitting of $55 \pm 10$ meV and *Thomann* [1999] obtained $47 \pm 6$ meV for 5 ML Co/Cu(100). Theoretical calculations also expect an exchange splitting in the order of 60 meV for ultrathin cobalt films [*van Gelderen et al.*, 1996]. The higher sample temperature (300 K) in this work cannot explain the deviation from the literature values because the Curie temperature is expected to be about 880 K [*Wu et al.*, 1996]. We want to note, however, that our technique explicitly uses spin resolution in contrast to the spin-integrated method of [*Wallauer and Fauster*, 1996, *Thomann et al.*, 2000] and [*Thomann et al.*, 1999].

From the bulk band structure one would expect an almost similar splitting of iron and cobalt ultrathin films since both materials show the same exchange splitting of the $d$ bands, which is about 1.2 eV [*Mankey et al.*, 1993]. Other studies even report on a larger exchange splitting of the $d$ bands of Co (1.55 eV) [*Clemens et al.*, 1992a]. A correlation between the exchange splitting of the image-potential states and of the $d$ bands in the bulk is limited due to two facts: Firstly, there is an enhancement of the magnetic moment in the surface layer [*Clemens et al.*, 1992a]. Secondly, the band gap situation still plays a major role. As explained in Section 2.1, the binding energy depends on the quantum defect, which itself is determined by the relative energetic position of the image-potential states in the projected band-gap. This directly affects the exchange splitting. For

a large binding energy one would in general also expect a large exchange splitting. Therefore, taking the exchange splitting of image-potential states as a sensor to compare the magnetic moment of different materials cannot be recommended.

However, one can use this sensor to compare the evolution of the surface magnetization e.g. with thickness. This has been done by *Thomann et al.* [1999] for 2-7 ML Fe/Cu(100). Weighting theoretical predicted layer-resolved magnetic moments [*Lorenz and Hafner*, 1996] with the penetration depth of the image-potential states could reasonably well describe the exchange splitting. In this work, no systematic measurements for different film thicknesses were made but a generally lower exchange splitting for a 7 ML Fe/Cu(100) film was obtained compared to 3 ML Fe/Cu(100) in accordance with [*Thomann et al.*, 1999]. This result reflects the two different magnetic states: a ferromagnetic film of 3 ML Fe/Cu(100) and an antiferromagnetic film with a 2 ML thick ferromagnetic cap-layer for 7 ML Fe/Cu(100).

## 5.2 Temperature dependence

### 5.2.1 Background

According to the power law, the decrease in the magnetization close to the Curie temperature $T_C$ is given by

$$M \propto \left(1 - \frac{T}{T_C}\right)^{\beta}, \tag{5.1}$$

where $\beta$ is the critical exponent and depends on the dimension of the real and spin space. In this section, we will study the spin polarization and the exchange splitting to monitor the temperature dependence of the magnetization. 7 ML Fe/Cu(100) serves as a test system.

With our technique we are sensitive to the electronic states and their spin. Therefore, before presenting the experimental results, a brief overview of the connection between the magnetization and the electronic band structure with focus on the temperature dependence will be given. More details can be found in [*Capellmann*, 1987].

For itinerant ferromagnets the bands in the ground state, i.e. $T = 0$ K, are exchange split according to their spins being aligned antiparallel or parallel to the macroscopic magnetization direction. At elevated temperature several extreme scenarios are usually considered, the most prominent ones described below:

- In the *Stoner model* [*Wohlfarth*, 1953] the exchange splitting is directly proportional to the magnetization. With increasing temperature the exchange splitting declines and drops to zero in the paramagnetic phase. This model was successfully introduced to explain the non-integer magnetic moments

of itinerant magnets. It failed, however, to describe the Curie temperatures, which are between 631 K and 1388 K for the $3d$ ferromagnets. In this section we will use the term *Stoner-like behavior* for a decrease of the exchange splitting with increasing temperature in general without referring to the microscopic origin.

- The *fluctuating-band theory* (FBT) [*Capellmann*, 1979, *Korenman et al.*, 1977] assumes that the change of the magnetization is caused by transverse fluctuations, like spin waves. These fluctuations may be considered as non-localized, uncoupled spin blocks. Due to their rapid oscillation ($10^{-13}s$) and small extent, a size of up to 20 Å was suggested [*Cappelmann*, 1982], they cannot be directly imaged. Evidence for the existence of magnetic moments above $T_C$ is given by the observation of spin waves [*Mook et al.*, 1973]. The extend of this short-range order is still large enough to support an exchange splitting, which is however defined with respect to the direction of the local magnetic moment.

Photoelectron spectroscopy or inverse photoemission experiments of $3d$ ferromagnets favor either the Stoner-like behavior or a constant exchange splitting of electronic states (see e.g. [*Schneider et al.*, 1991b] or [*Donath and Dose*, 1989]). Some experiments also report on a mixture of both [*Hopster et al.*, 1983] or a different behavior for certain bands [*Kirschner et al.*, 1984].

What consequences do these two models have in general on a 2PPE spectrum? The exchange splitting and the linewidth reflect properties of the image-potential states whereas the spin polarization and intensity give information about the initial states.

Let us only consider the $n$=1 image-potential state so far. Since the exchange splitting is smaller by a factor of two than the linewidth, spin resolution is necessary to distinguish between the majority and minority states. A Stoner-like behavior of the image-potential state would lead to a decrease in exchange splitting with increasing temperature, which would be directly visible in the spin-resolved spectra. At and above the Curie temperature the exchange splitting is zero. In the integrated spectra one expects simply a decline in the linewidth up to the Curie temperature. The different spin-dependent linewidths approach each other at $T_C$ since no spin dependence exists in the paramagnetic phase.

In the framework of the FBT the exchange splitting is not affected by temperature. However, the local spin direction does not coincide any more to the axis defined by the spin-polarization detector. In the spectrum this leads to a mixing of the spin components in the exchange-split states. Since the linewidth is much larger than the exchange splitting, the latter cannot be observed directly, which means that the spectrum never shows two separated peaks. Only the spin resolution allows us to distinguish the exchange split states. Because of the spin mixing at elevated temperatures even in a spin-resolved measurement one spin

component cannot solely be ascribed to one of the exchange split states. This leads to an apparent converging of the exchange-split states in the measurements which ends up in equivalent peak positions at $T_C$. This shift could be wrongly interpreted as a decrease of the exchange splitting.

Simultaneously, the spin-dependent linewidths should increase close to $T_C$, since both states contribute to the measured majority and minority spin component. To which value the linewidth rises at $T_C$ depends on the spin-dependent linewidth, intensity and exchange splitting. The spin-integrated linewidth should not be affected at all. In this case always both states are measured, below and above $T_C$. The impact of the two models on a 2PPE spectrum is illustrated in Figure 5.1.

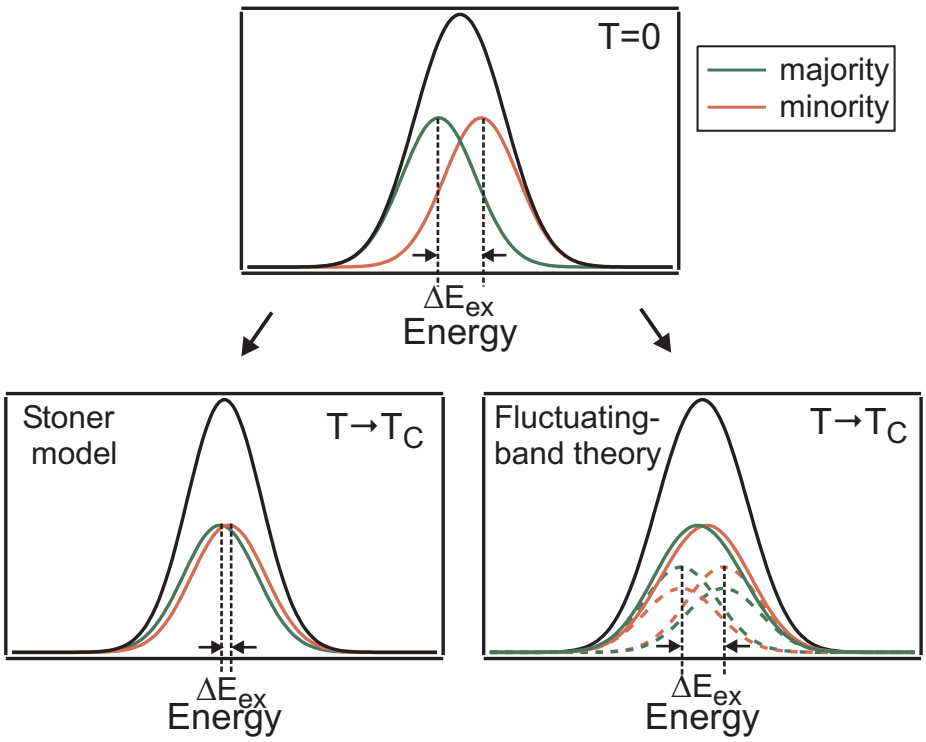


**Figure 5.1**: *Gedanken experiment of spin-resolved 2PPE spectra of ferromagnetic systems at T=0 K and at temperatures slightly below $T_C$ for two different scenarios. The lower left panel shows a Stoner behavior where the exchange splitting decreases with increasing temperature. The spectra in the lower right panel reflect the FBT, where the exchange splitting is constant with increasing temperature but the spin of these states depolarize with respect to the axis defined by the spin-polarization detector.*

By assuming a small exchange splitting compared to the linewidth the most important consequences of the two models on the temperature dependence of image-potential states in a spin-resolved 2PPE can be summarized as follows:

Stoner-model:

- Decrease of the exchange splitting with increasing temperature and a collapse to zero at $T_C$
- Decrease of the spin-integrated linewidth
- Approach of majority and minority state linewidth

Fluctuating band theory:

- Apparent decrease of exchange splitting in spin-resolved measurements
- Constant spin-integrated linewidth
- Increase of spin-dependent linewidth at $T_C$

### 5.2.2 Results

These considerations are enough to present and discuss the results in detail. A measure for the magnetization will be the exchange splitting, the spin polarization and the linewidth . Additionally, one can use spin-integrated 2PPE to deduce the presence of an exchange splitting [*Wallauer and Fauster*, 1996, *Thomann et al.*, 2000, 1999]. Switching from p- to s-polarized light leads to a change of the relative spin population of the IPS due to the dipole selection rules (see also Section 4.2.1). As displayed in Figure 5.2 a peak shift in the spin-integrated spectrum can therefore be observed. This quantity $\Delta E_{p-s}$ will now also be used as a measure for the presence of an exchange splitting. One could now also try to deduce the exchange splitting by a two peak fit as it was first done by [*Wallauer and Fauster*, 1996]. This method, however, is based on the assumption that the s-polarized spectrum is purely positively spin-polarized, which is not exactly valid for the studied system, a 7 ML iron film on Cu(100) pumped with a 4.43 eV laser pulse.

The temperature-dependent measurements were taken at a slight pump-probe delay of about 10 - 20 fs, which had the advantage of higher count rates and a smaller peak width compared to measurements taken at zero pump-probe delay as discussed in Section 2.2. Starting from 335 K, spectra were recorded for p- and s-polarized light down to 252 K. As a crosscheck the last measurement was performed at 330 K to exclude any changes with time. A systematic error of about 3 K in the temperature reading has to be included, which does not influence any of the results except for a temperature offset.

The spectra obtained for p-polarized light are shown in Figure 5.3. Below 270 K, the states are clearly exchange split and only a small decrease in spin polarization with increasing temperature is visible. Between 270 K and 273 K the exchange splitting and the spin polarization drops to zero. Above 273 K no

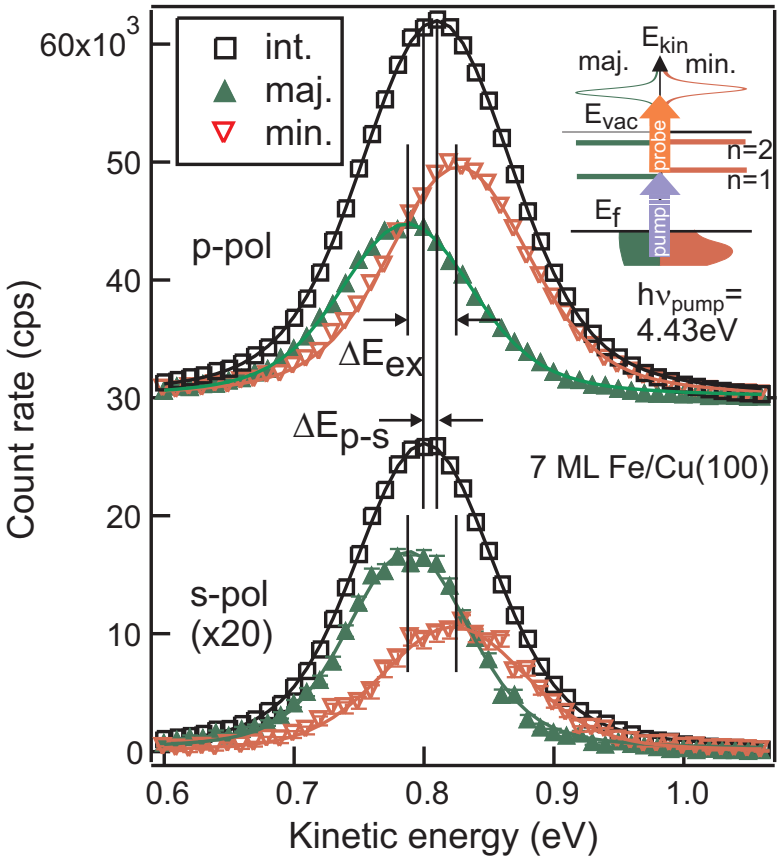


**Figure 5.2**: *Temperature-dependent quantities, which can be deduced from spin-resolved and spin-integrated 2PPE spectra: Exchange splitting ($\Delta E_{ex}$), linewidth, energetic difference between p- and s-polarized peak maxima of spin-integrated spectra ($\Delta E_{p-s}$) and spin polarization ($P$). The data is taken from a 7 ML Fe/Cu(100) film at 252 K. The inset illustrates the excitation process for spin-resolved 2PPE.*

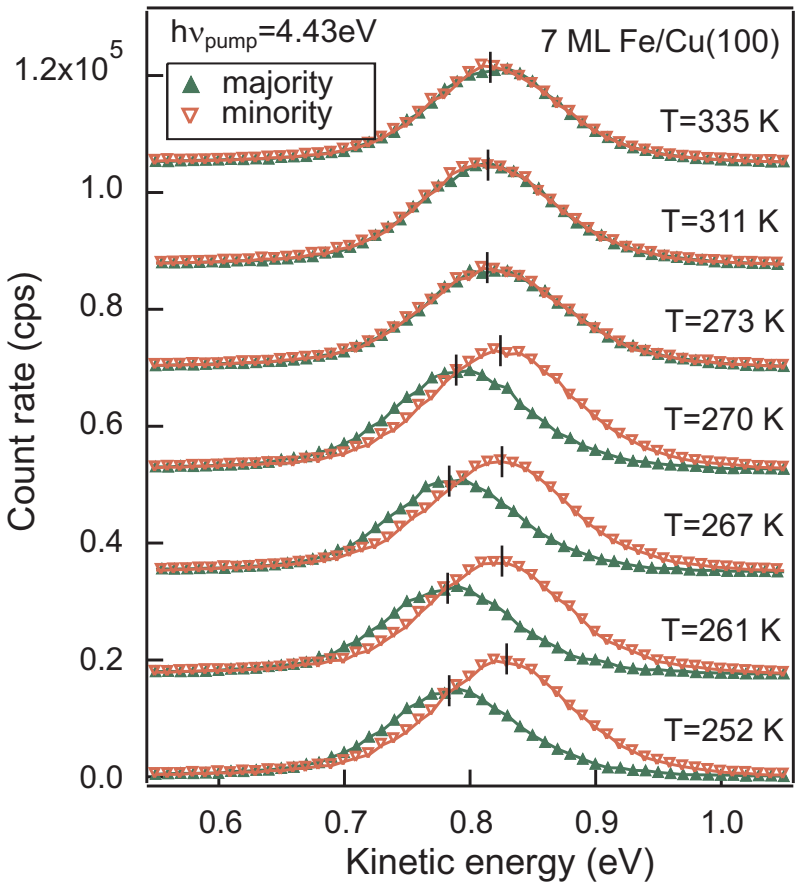


**Figure 5.3**: *Temperature dependence of spin-resolved 2PPE spectra for 7 ML Fe/Cu(100). The pump pulse for these measurements was p-polarized and had a photon energy of 4.43 eV.*

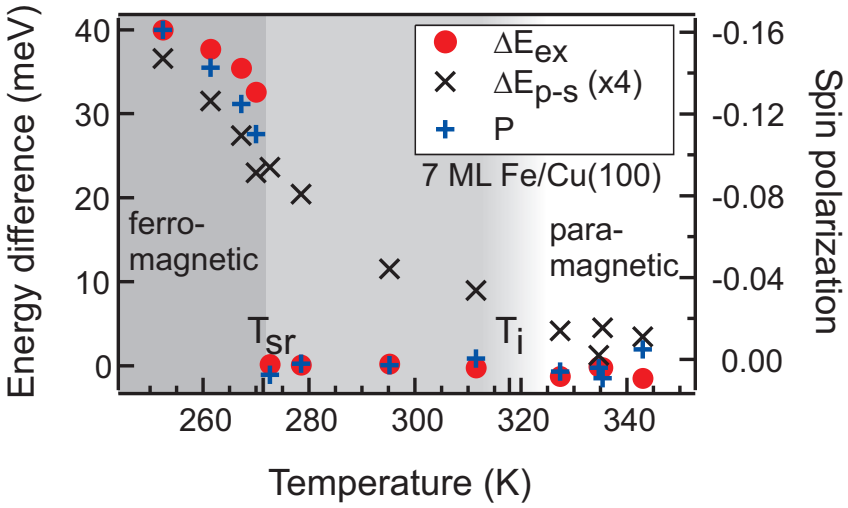


**Figure 5.4**: *Different temperature behavior of the exchange splitting ($\Delta E_{ex}$), spin polarization ($P$) and pump-pulse polarization induced peak shift ($\Delta E_{p-s}$). $T_{sr}$ marks the temperature at which $\Delta E_{ex}$ and $P$ vanishes whereas $T_i$ corresponds to the temperature where $\Delta E_{p-s}$ is becoming constant at about 0 meV.*

strong changes can be observed. In general only the $n$=1 state is excited due to the small pump-pulse photon energy.

In this paragraph, we will quantify the temperature-dependent changes. In Figure 5.6 the exchange splitting $\Delta E_{ex}$, the spin polarization $P$ and the peak shift between the integrated spectra obtained with p- and s-polarized light $\Delta E_{p-s}$ are shown. As we have already discussed, $\Delta E_{ex}$ and $P$ slightly decrease with temperature and drop rapidly to zero at temperature of about $T_{sr}$=270 K[1]. This suggests a phase transition to the paramagnetic phase. Therefore, at first glance, an assignment of $T_{sr}$ to the Curie temperature seems reasonable. The temperature behavior of $\Delta E_{p-s}$, however, shows a completely different evolution. It slowly reduces from about 8 meV to 0 meV between 252 K and 340 K. No sudden drop at $T_{sr}$ is observed, which contradicts the idea of a magnetic phase transition at this temperature. The Curie temperature is supposed to be in a region between 310 K and 330 K where $\Delta E_{p-s}$ is approximately 0 meV. This temperature region is assigned with $T_i$ in Figures 5.4 and 5.5 [2]

To clarify this difference one may now also look at the evolution of the linewidth, plotted in Figure 5.5. Below $T_{sr}$ a spin-dependent linewidth can be observed, whose difference can be ascribed to the spin-dependent lifetimes and dephasing rates [*Schmidt et al.*, 2005]. Above $T_{sr}$ any spin dependence is lost, therefore both linewidths are equal to the integrated linewidth. Particularly, at

[1]The subscript *sr* is used as a abbreviation for spin resolved.
[2]The subscript $i$ denotes (spin-)integrated.

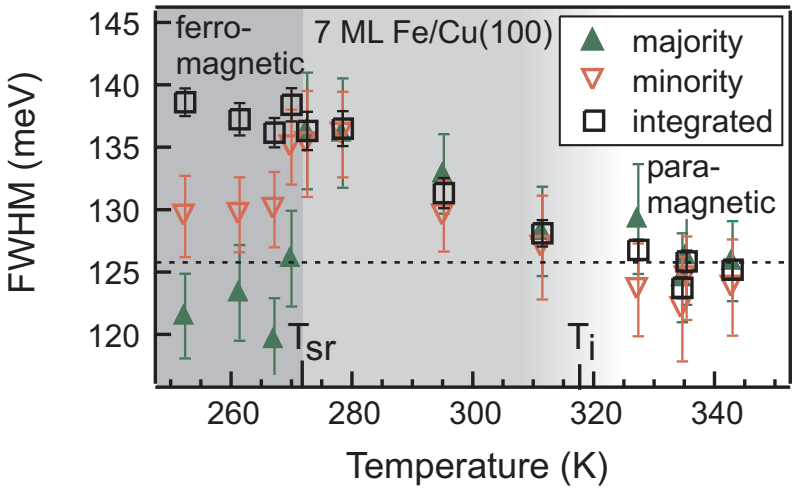


**Figure 5.5**: *Evolution of spin-resolved and spin-integrated linewidth with temperature. $T_r$ indicates the temperature at which spin resolution has vanished. At $T_i$ the integrated linewidth converges to a value which is between the linewidth of the spin resolved peaks, which is indicated by the horizontal line.*

$T_{sr}$ the integrated linewidth is larger than the spin-dependent linewidths, slightly below $T_{sr}$. With increasing temperature it decreases and ends up at a value which is between those for the majority and minority linewidths. At this point one has to emphasize that a linewidth broadening with temperature due to phonon interaction can be neglected because of the small overlap of the image-potential states with the bulk [*Eiguren et al.*, 2003]. This facilitates a temperature-dependent study of these electronic states considerably compared to the study of bulk states.

Although the use of $\Delta E_{p-s}$ and the linewidth as a measure for the exchange splitting is convincing, one limiting fact has to be considered. With increasing temperature the work function decreases and therefore also the binding energy of the image-potential states with respect to the Fermi level becomes smaller. This is demonstrated in Figure 5.6 where the energy of the $n$=1 image-potential state is plotted for different temperatures. A change in the integrated binding energy of about 40 meV between 260 K and 340 K can be observed. Due to the constant photon energy, the initial-state energy in the 2PPE process is shifted accordingly. It has already been demonstrated in Section 4.2.2 that the distribution of the initial states is not constant. Therefore a change of the initial-state energy leads to variation of the spin polarization. This, however, causes a slight shift of the center of mass in the spin-integrated spectrum and therefore influences $\Delta E_{p-s}$ and also the integrated linewidth.

To estimate the contribution of this initial-state shift one measurement was performed at 260 K with a pump-pulse photon energy of 4.48 eV (about 50 meV larger than in the previous measurement). The initial-state energy for the mea-

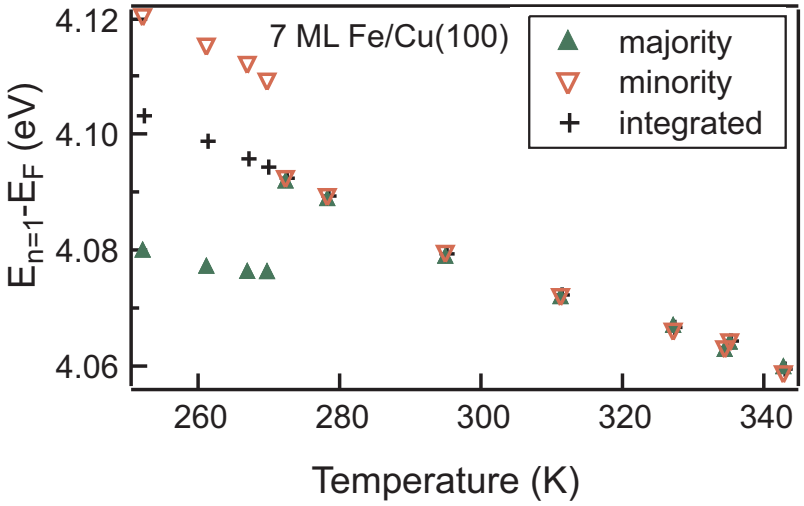


**Figure 5.6**: *Dependence of the binding energy on the temperature. Note that the energy scale refers to the Fermi level, so that the change in binding energy is governed by the temperature dependent work function.*

surement at 260 K and $h\nu_{pump} = 4.48$ eV corresponds roughly to the initial-state energy of the measurement at 340 K and $h\nu_{pump}$= 4.43 eV in Figure 5.4. Therefore, the two values of $\Delta E_{p-s}$ can be directly compared. For the measurement with a photon energy of 4.48 eV $\Delta E_{p-s}$ amounts up to 4 meV, and is considerably smaller than 8 meV as obtained for $h\nu_{pump} = 4.43$ eV (see Figure 5.4). Nevertheless, the drop to about 0 meV of the corresponding measurement at 340 K proves the reduction of magnetization. It has to be noted that a vanishing $\Delta E_{p-s}$ in the paramagnetic phase is not a must. The initial states still influence the energetic position of the peak maximum observed in 2PPE for overlapping pump-and probe pulses as discussed in Section 5.1. Since the electronic structure of states with $\Delta_5$ representation differs from the distribution of $\Delta_1$ states, a difference is possible for measurements with p- and s-polarized light.

So far we have left out the temperature dependence of the initial states in the presentation of the results. As mentioned above, their influence enters in the spin polarization and the intensity of the image-potential states. The spin polarization can be deduced from the spin-resolved spectra directly. The shift of the spin-integrated peak with light polarization ($\Delta E_{p-s}$) requires an exchange split image-potential states and a spin-dependent excitation which depends on the light polarization. Since the latter is an initial-state effect, $\Delta E_{p-s}$ can also be used as a measure for changes in the initial-state distribution. The evolution of $\Delta E_{p-s}$ (see Figure 5.4) indicates that there is no sudden change at $T_{sr}$ but a slow decrease up to $T_i$. As explained above this quantity is also influenced by the temperature dependent work function.

It is not reasonable to discuss the intensity of the image-potential states in the

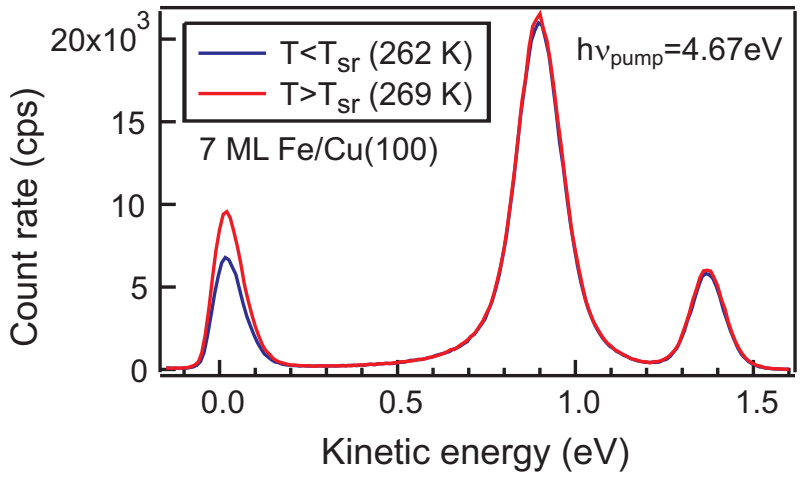


**Figure 5.7**: *Equivalence of spin-integrated 2PPE spectra of a 7 ML Fe/Cu(100) film below and above $T_{sr}$. The spectra were taken at a pump-pulse energy of 4.67 eV so that the $n = 2$ was also populated. The transition temperature was in this preparation about $T_{sr} = 265$ K.*

spectra over a broad temperature range for two reasons. Firstly, the experiment doesn't provide a stable laser power for several hours, which is the necessary time to record a series of spectra for different temperatures. Secondly, the shift of the work function leads to changes of the initial states. This only allows one to compare data in a limited temperature range. In Figure 5.7 two spin-integrated 2PPE measurements are plotted, one spectrum was recorded slightly below and the other slightly above $T_{sr}$. The photon energy was large enough ($h\nu_{pump} =$ 4.67 eV) to excite the $n$=2 image-potential state. One notifies that there is no difference in intensity, which means that the initial state band-structure has not changed at $T_{sr}$ with respect to its energy distribution.

To sum up the spin-resolved measurements favor a Curie temperature at $T_{sr}$ due to the vanishing spin polarization and the respective decline of the exchange splitting.

The results from spin-integrated measurements, however, are at variance with such a low Curie temperature and suggest $T_i$ to be the real Curie temperature. Furthermore, for the image-potential states a Stoner-like behavior from the linewidth evolution can be deduced. At the temperature $T_i$, it is between the value obtained for the majority and minority state.

The spin-integrated measurements also suggest that the initial states are still spin polarized and do not change their distribution at $T_{sr}$.

### 5.2.3 Interpretation

The two seemingly contradictory results can be understood as follows: The data is averaged spatially and temporally over spin blocks which can be thought of either fluctuations according to FBT or of magnetic domains. This averaging causes a loss of the spin polarization but doesn't affect the spin-integrated intensity.

This statement bases on the assumption that the extent of the image-potential states is smaller than the size of the spin block or domain. *Fischer et al.* [1993b] have already addressed the problem of the spatial extension of the $n$=1 image-potential state in a 2PPE experiment, where small Ag islands were grown on Pd(111). It was shown that the $n$=1 image-potential state could already exist on island with sizes down to 10 Å in diameter. In agreement to this it could also be shown for stepped Cu(100) that for a terrace width of 19 Å the parallel component of the wave vector of the $n$=1 image-potential state is defined to the terrace surface. In contrast the $n \geq 2$ image-potential states are still related to the macroscopic surface.

The two possible interpretations base on the localization of the image-potential states on a magnetic domain or a spin block and will now be discussed in more detail

#### Multi-domain formation

By assuming that the real Curie temperature is indeed $T_i$ the loss of spin polarization at $T_{sr}$ can be interpreted as a transformation to a multi-domain state, which is in some cases the ground state for an *out-of-plane*-magnetized two-dimensional ferromagnet [*Yafet and Gyorgy*, 1988]. This also explains the negligible change of the integrated spectra in Figure 5.7 below and above $T_{sr}$ in a new manner. Since there is no magnetic phase transition no change is expected in the spin-integrated spectrum. The transition to a paramagnetic state should be somewhere around $T_i$, where $\Delta E_{p-s}$ is becoming small and the spin-integrated linewidth has declined to a value between the majority and minority linewidths at a temperature below $T_{sr}$.

A two dimensional film with out of plane magnetization may decay into magnetic domains at elevated temperatures. This can be explained by the competition between the exchange coupling, which favors a parallel alignment of spins and the dipolar coupling, which favors a decay into domains to avoid magnetic stray fields. With increasing temperature the strength of the exchange interaction is overcome by the long range dipolar coupling.

Early experiments with MOKE on 7.5 ML Fe/Cu(100) obtained a Curie temperature of $T_C$=273 ±3 K but did not consider the formation of domains [*Thomassen*, 1993]. From appearance potential spectroscopy on 7 ML Fe/Cu(100) a Curie temperature of $T_C$ = 280 K was deduced (see Figure 1 in [*Detzel et al.*, 1995]) but after cooling the sample from a temperature close to $T_C$ the mea-

sured magnetization did not recover. By remagnetizing the sample the initial magnetization was again observed. This was interpreted as a decay of the film at elevated temperatures into domains which act as superparamagnets. Therefore the deduced Curie temperature was interpreted as a maximum blocking temperature of the largest domain. This also explained the linear decrease of magnetization which was observed in this experiment and also in temperature dependent measurements of the spin polarization by [*Pescia et al.*, 1987]. This temperature behavior, however, contradicts other investigations including ours. Superparamagnetism therefore is unlikely to be the cause of the sharp decline at $T_{sr}$.

Spin-polarized metastable-atom deexcitation spectroscopy (SPMDS), which is a very surface sensitive technique, and a MOKE study revealed a Curie temperature of $T_C$=264 K [*Kurahashi et al.*, 2003b]. A sharp drop-off at this temperature was ascribed to a 2D-Ising-like behavior. Later, this study was refined [*Kurahashi et al.*, 2003c] and a decrease of the magnetization within some seconds was observed for temperatures in the range of $T_C$ - 5 K $< T < T_C$. This instability was attributed to a relaxation into an energetically favorable multi-domain state. Here we have to note that data recording took about 4 minutes for the p-polarized measurements and 16 minutes for the s-polarized measurements in the present experiment. The possible temporary existence of a macroscopic magnetization on a second timescale in the region between $T_{sr}$ and $T_i$ was checked by measuring the spin polarization versus real time at one specific kinetic energy where a strong spin polarization would be expected. We did not observe any spin polarization after applying the magnetization pulse. However, we are limited with realtime resolution to about 2 seconds. Furthermore, we did also not observe any spin polarization in the *in-plane* direction, which rules out a possible spin reorientation.

*Vollmer et al.* [2000] also recognized a sharp drop-off in the remanent magnetization at about 280 K but realized that the inflection point of the magnetization curve in saturation is shifted approximately 20 K upwards compared to the magnetization curve in remanence. This was attributed to domain formation, which has also been observed with MOKE on *out-of-plane* magnetized nickel films on Cu(100) [*Poulopoulos et al.*, 1997]. Here a drop-off of the remanent magnetization 20 K below $T_C$ was reported. It was also pointed out that measuring the magnetization in remanence not only leads to a wrong assignment of $T_C$ but also to an erroneous determination of the critical parameter. To remove the domain structure a magnetic field $\vec{H}$ has to be applied and $\vec{M}$ has to be extrapolated to $\vec{H} = 0$.

To completely bypass the problem of magnetic-domain formation a magnetic imaging experiment would be necessary. Measurements with spin-polarized low energy electron microcopy (SPLEEM) deduced a Curie temperature of about 250 K for 5.5 ML Fe/Cu(100) (Figure 7 in [*Man et al.*, 2001b]). This value is even slightly lower than the temperature which is assumed for the domain formation

by [*Vollmer et al.*, 2000] and therefore contradicts the idea of the true Curie temperature being far above 280 K. The different film thickness cannot explain this contradiction, since for a 5 ML iron film the Curie temperature is even slightly larger than for 7 ML Fe/Cu(100) [*Thomassen*, 1993]. As discussed in Section 2.3.1 ultrathin iron films on Cu(100) are an extremely sensitive structure. A slight difference in the preparation might have a serious impact on the magnetization behavior. *Man et al.* [2001b] showed in their SPLEEM study that the growth rate has a strong influence on the Curie temperature. For low deposition rates an even smaller $T_C$ was obtained. Furthermore, structural changes during heating may evolve which govern the magnetization behavior as observed for 4 ML Fe/Cu(100) [*Zharnikov et al.*, 1996]. No strong differences in preparation in the experiment from [*Man et al.*, 2001b] to this experiment exist and therefore preparation effects should be small. This result contradicts, so far, the interpretation of a domain formation at $T_{sr}$.

An open point is the question about the size and shape one may expect for these domains. The SPLEEM measurements [*Man et al.*, 2001a] revealed a stripe pattern in analogy to SEMPA (scanning electron microscopy with polarization analysis) experiments on Fe/Cu(100) with a thickness below 5 ML [*Vaterlaus et al.*, 2000]. Both experiments observed a breakup into smaller domains with increasing temperature. The SEMPA experiment additionally observed a break-up of these stripes into pieces which was ascribed to a melting into a "tetragonal liquid crystal"-phase which was already predicted by [*Abanov et al.*, 1995]. As the authors pointed out, the region with zero polarization in their experiment could still be caused by mesoscopic domains which fluctuate on a timescale smaller than the timescale of the experiment (5 min). Furthermore, domains smaller than the spatial resolution (20nm) could not be detected. The spatial resolution of SPLEEM is theoretically about 10 nm [*Grzelakowski and Bauer*, 1996] and therefore might face the same problem. One may also think about a spatial fluctuation of the domain pattern [*Czech and Villain*, 1989]. Mobile stripes were indeed observed in a recent experiment [*Portmann et al.*, 2006].

Although, in our case, the film is 7 ML thick it is still comparable to a two dimensional system, since only the top two layers are ferromagneticly coupled. For the antiferromagnetic structure beneath a Néel temperature of $T_N$=200 K was determined by MOKE measurements [*Li et al.*, 1994]. Therefore, we can assume that we indeed have an almost pure two dimensional system in the studied temperature range.

To summarize this interpretation, we have at $T_{sr}$ a break-up in domains, which causes the loss of spin-polarization and therefore mimics a magnetic phase transition. With increasing temperature, these domains decay into smaller ones. Whether these domains show a stripe pattern or represent the "tetragonal liquid crystal"-phase remains open. The decreasing size, possible fluctuations and the real transition into the paramagnetic phase lead to a decrease of the exchange

splitting of the image-potential states as observed by the evolution of $E_{p-s}$ and the integrated linewidth.

The whole discussion about a phase transition of the domain structure with fluctuations and very small domain sizes brings us close to the second possible interpretation.

### Magnetic moments above the Curie Temperature

The other possibility to explain the discrepancy in the observed transition temperatures $T_{sr}$ and $T_i$ is provided by the fluctuating-band theory. In this case $T_{sr}$ is the real Curie temperature. For larger temperatures local magnetic moments with a spatial extent of 10 - 20 Å on a timescale of 100 fs may still exist [*Capellmann*, 1987]. As explained above the size of the $n$=1 image-potential state is in the range of 20 Å and its lifetime is below 20 fs for ultrathin iron films on Cu(100) [*Schmidt et al.*, 2005]. Therefore, the $n$=1 image-potential state could still be locally exchange split on one spin block within its lifetime. In this manner the image-potential states can be understood as a local magnetic probe on a femtosecond timescale. At elevated temperatures the spin blocks become small which leads to decrease of the exchange splitting as observed in our measurements

### Concluding remarks

The results can be summarized as follows. At $T_{sr}$ the single domain state becomes unstable and therefore leads to a loss of a macroscopic spin polarization. The question whether this is due to multi-domain formation or this can be understood as fluctuation of local magnetic moments in time and space remains still open. Since the domain formation of ultrathin iron films on copper is evinced by MOKE measurements [*Vollmer et al.*, 2000] and also by imaging techniques like SEMPA [*Vaterlaus et al.*, 2000] the interpretation of $T_{sr}$ being the temperature of a decay in a multi domain state seems more reasonable.

The success of the present measurement is that image-potential states can be used as a local sensor for magnetization. Processes which mimics a magnetic phase transition can be revealed. To follow the magnetization to deduce the critical exponent (see Equation 5.1) or even to prove undoubtedly the existence of local magnetic moments above $T_C$, measurements would be necessary on a magnetic system where no domain transition is expected. In this manner *in-plane* magnetized films would be good candidates, like ultrathin cobalt films on Cu(100).